# Single- and Multilayers of Alkali Metal Atoms Inside Graphene/$MoS_2$ Heterostructures: a Systematic First-Principles Study

Chepkasov, I. V.; Smet, J. H.; Krasheninnikov, A.;

Originally published:

September 2022

**Journal of Physical Chemistry C 126(2022), 15558**

DOI: https://doi.org/10.1021/acs.jpcc.2c03749

# Single- and Multi-Layers of Alkali Metal Atoms Inside Graphene/$MoS_2$ Heterostructures: a Systematic First-Principles Study

Ilya V. Chepkasov,[*,†] Jurgen H. Smet,[‡] and Arkady V. Krasheninnikov[*,†,¶]

†*Institute of Ion Beam Physics and Materials Research, Helmholtz-Zentrum Dresden-Rossendorf, D-01328 Dresden, Germany*

‡*Max Planck Institute for Solid State Research, D-70569 Stuttgart, Germany*

¶*Department of Applied Physics, Aalto University, P.O. Box 11100, FI-00076 Aalto, Finland*

E-mail: ilya_chepkasov@mail.ru; a.krasheninnikov@hzdr.de

**Abstract**

Stacking various two-dimensional (2D) materials in van der Waals (vdW) heterostructures is a novel approach to design new systems, which can host alkali metal (AM) atoms to tune their electronic properties or store energy. Using state-of-the-art first-principles calculations, we systematically study the intercalation of the most widespread AMs (Li, Na, K) into a graphene/$MoS_2$ heterostructure. Contrary to previous work on the intercalation of AMs into various heterostructures based on 2D materials, we consider not only single-, but also multi-layer configurations of AM atoms. We assess the intercalation energetics for various concentrations of AM atoms, calculate charge transfer from AM atoms to the host system, and show that although intercalation of AMs as single layer is energetically preferable, multi-layer configurations can exist at high concentrations of AM atoms. We further demonstrate that the transition

of the $MoS_2$ layer from the $H$ to $T'$ phase is possible upon Li intercalation, but not Na or K. Our findings should help to better understand the behavior of heterostructures upon AM atom intercalation and may stimulate further experiments aimed at the tailoring of heterostructure properties and increasing the capacity of anode materials in AM ion batteries.

# Introduction

The intercalation of alkali metal (AM) atoms into layered bulk and low-dimensional materials has recently received an enormous amount of attention in the context of energy storage[1–3] and tuning the opto-electronic properties of the materials.[4–6] As for the former, increasing the capacity of metal-ion batteries is believed to be crucial for further development of portable electronics and electrical vehicles. One of the promising directions of improving the characteristics of metal-ion batteries, such as the capacity and the critical number of cycles, is the use of composites as anodes.[7–10] Among these systems, van der Waals heterostructures consisting of stacked layers of graphene and transition metal dichalcogenides (TMDs), such as $MoS_2$, have attracted particular attention[11–14] as perspective metal-anode materials. $MoS_2$ has low electronic conductivity and undergoes a strong volume change upon intercalation/deintercalation, but intercalation of AMs into these systems is energetically more favorable as compared to graphitic structures,[15] so that a combination of $MoS_2$ with conductive carbon matrices is expected to be a promising direction. In particular, $MoS_2$/graphene heterostructures were synthesized,[11–14] and demonstrated to be promising systems as anode materials in lithium ion batteries exhibiting extraordinary capacity (up to 1300 $mAhg^{-1}$) and excellent rate capability and cycling stability.

With regard to tailoring characteristics of heterostructures, Li intercalation into electrochemical devices based on stacked hexagonal boron nitride, TMDs, and graphene layers has been demonstrated to be an effective approach to control the electronic and optical properties of such systems.[4] As for $MoS_2$/graphene heterostructures, intercalated Li atoms have

been found to increase the electronic conductivity and electrochemical performance of these systems.[11–13]

The AM intercalation into heterostructures has also been theoretically investigated. Specifically, studies focused on the intercalation of AMs into $MoS_2$/graphene and other heterostructures have addressed the stability, charge transfer, and electronic structure of these systems.[15–18] In particular, it was shown that intercalation of Li between Gr/$MoS_2$ layers is energetically more favorable over adsorption on either side[15] of the structure. It was also shown[17] that an increase in the concentration of intercalated Li atoms in Gr/$MoS_2$ composite leads to band gap opening in graphene. Larson et al. studied the intercalation of lithium atoms into Gr/$MoS_2$ heterostructures with different $MoS_2$ phases ($H$ and $T'$) and determined that the morphology of $MoS_2$ does not significantly affect the stability, Li diffusion barrier and charge transfer.[18]

Na intercalation into hybrid structures has been studied as well,[19–22] as Na-ion batteries, if developed, are expected to be economically and environmentally much more attractive than Li-ion batteries. Massaro et al.[23] carried out first-principles calculations aimed at the investigation of sodium intercalation between graphene and $MoS_2$ layers, and assessed the electronic properties and possible diffusion paths of Na atoms along the interfaces, and estimated the corresponding energy barriers. In addition to Na, K has also been actively considered as an alternative to Li. Recently, the possibility of creating K-ion battery has been intensely studied.[24,25] Zhang et al. investigated K and Li intercalation into N-doped graphene/$MoS_2$ ($2H$ and $1T$) and showed that doping plays a vital role in improving the structural stability of Gr/$MoS_2$ structures.[26]

However, many aspects of AM intercalation in heterostructures remain not fully understood. In particular, the energetics and possible phase segregation of AM atoms as a function of their concentration have not been studied for Na and K. Many investigations were focused on bulk structures, not Gr/$MoS_2$ bilayers, while recent experiments demonstrated that formation of multi-layer Li structures is possible in bi-layer graphene.[27] Calculations

also predict that this should be possible for some AMs (at least Li and K) intercalated into $MoS_2$ bilayer.[28]

In this work, we systematically study the intercalation of Li, Na, and K into a Gr/$MoS_2$ bilayer heterostructure using first-principles calculations. We consider both single and multi-layer AM configurations, and investigate the energetics related to the stability of the system for various concentrations of AMs. We further address the charge transfer and possible transformation of $MoS_2$ from the $H$ to $T'$ phase.

## Simulation methodology

All our calculations were carried out within the framework of the density-functional theory (DFT) as implemented in the VASP software package.[29,30] An energy cut-off of 600 eV was used for the supercell calculations. The Brillouin zones of the primitive cells of the 2D materials and bulk AMs were sampled using a 12×12×1 and 12×12×12 Monkhorst–Pack grid points.[31] A Γ-centered k-point $5 \times 5 \times 1$ sampling was used in the supercell calculations. The maximum force on each atom was set to be less than 0.01 eV for the geometry optimization. All calculations were performed on a $5 \times 5$ graphene $4 \times 4$ $MoS_2$ periodic supercell structure, consisting of 98 atoms. The concentration of Li, Na, K atoms changed either from 1 to 16 (for Na and K) or to 19 (for Li). Dipole corrections were not used in the calculations, but test runs with account for the corrections gave the values of the total energy being different by less than 0.01 eV. The atomic structures and the charge densities were visualized using the VESTA package.[32] At least 20Å of vacuum was used along the direction perpendicular to the layers (z-axis) to prevent spurious image interaction. To build the Gr/$MoS_2$ structures with multi-layered AMs, we used the Virtual NanoLab software.[33] The typical atomic configurations for single and multi-layer AM structures are presented in Fig. 1.

To estimate the energetics directly related to the stability of different configurations, we calculated the intercalation energy $E_i$ per AM atom, corresponding to the energy change

when $n_{AM}$ AM atoms are moved from the bulk AM crystal into the heterostructure. It is defined as

$$E_i = [E(n_{AM}) - E(0)]/n_{AM} - \mu_{AM}. \quad (1)$$

Here $E(n_{AM})$ is the total energy of the Gr/H-$MoS_2$ system with $n_{AM}$ AM intercalated atoms, $E(0)$ is the energy of the pristine Gr/$MoS_2$ structure, and $\mu_{AM}$ is the chemical potential of the AM atom in the bulk structure (HCP for Li, Na, K).

We also considered the reaction energy, $E_r$, the average gain or loss for adding one AM atoms from the system. It is defined as

$$E_r = E(n_{AM} - 1) + \mu_{AM} - E(n_{AM}), \quad (2)$$

This is essentially the derivative of $E_i$ with regard to $n_{AM}$. A positive value indicates that it is energetically favorable for additional AM atoms to be close to the existing AM structure. Negative values suggest that the intercalated AM atoms tend to be spatially separated.

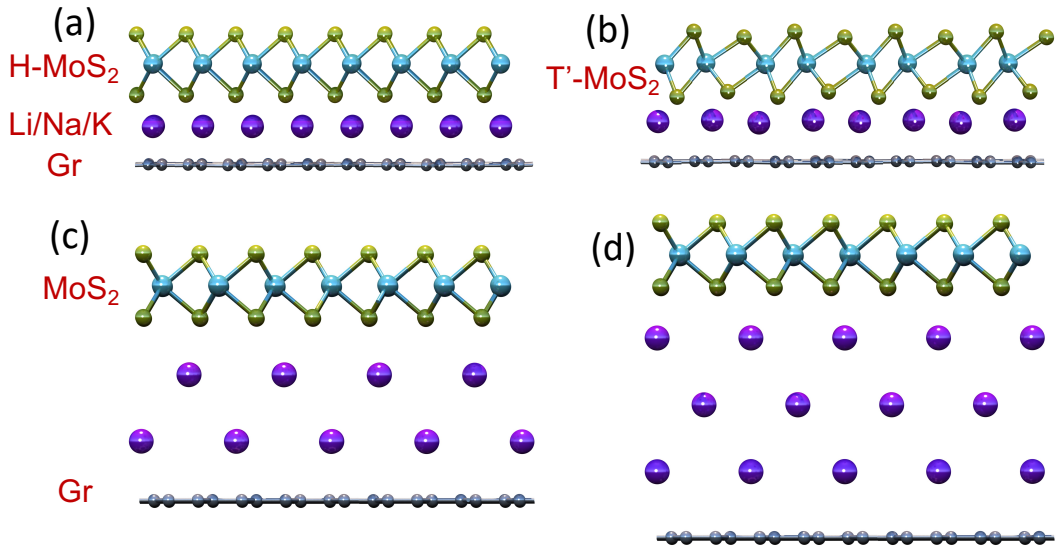


Figure 1: Typical atomic configurations illustrating the single and multilayer structures of alkali metals (AMs) between the sheets of the host material, graphene (Gr) and $MoS_2$. (a,b) Single layer of AMs in the Gr/$MoS_2$ heterostructure with $MoS_2$ being in the $H$ or $T'$ phase, respectively. HCP bilayer AM (c) and FCC trilayer (d) configurations in the Gr/$MoS_2$ heterostructure.

## Results and discussion

Prior to assessing the intercalation energy, we carried out the calculations to study the dependence of the results on the choice of the method to describe the van der Waals (vdW) interaction. The proper account for vdW interactions is highly important when simulating multi-layer 2D materials and heterostructures ,[34–36] with and without intercalated species. Specifically, the interlayer separation in the pristine system may change,[35] thus offering more or less space available for the intercalation. Moreover, the electronic properties, e.g. the gap in the electronic spectrum may also substantially change, as demonstrated, e.g., for platinum dichalcogenides.[37] The methods for the calculation of the vdW interaction can be divided into three categories: semiempirical models suggested by Grimme et al.,[38–40] models based on the atomic polarization modified by the electron density,[41–44] and full density functional approximations based on pairwise dispersion models using only the density.[45,46] The analysis of the methods for the prediction of the geometric and energy properties of various 2D materials (including graphene and $MoS_2$) was done by Tawfik et al.[36] Four of the eleven methods considered (MBD@rsSCS/FI+ER,[44] DFT-D3,[39] optB88-vdW,[47] and DFT-dDsC[43]) provide higher accuracy as compared to other methods. Also, the work of Tawfik et al.[36] reported that the most accurate method for a description of chemical and dispersion forces in 2D materials is SCAN+rVV10.[48] However, a critical issue with SCAN+rVV10 is its computational performance. We used several methods for calculating the vdW forces. The results of our calculations ($\mu_{Li}$, $E_i$ and the average charge transfer from Li atoms to the host material) for 16 Li atoms in the system are listed in Table 1. All methods gave almost the same charge transfer(0.83-0.85 $e^-$), but the calculated $E_i$ was quite different for different methods. For example in the case of DFT-TS and DFT-TS/HI methods, the formation energy is positive because this method yields $\mu_{Li}$ (for the bulk HCP structure taken as the reference) approximately two times lower than other methods, which was also shown previously.[49] Hence, taking into account the good prediction of the energy (as compared to other more accurate methods), and lattice parameter of 2D materials, as well as computational performance, we

used the zero damping DFT-D3 method of Grimme[39] in our calcualtions.

Table 1: The computational methods used, chemical potential of Li atom in the bulk structure $\mu_{Li}$, intercalation energy $E_i$ and charge transfer using the Bader analysis[50] in a $Gr/MoS_2$ bilayer heterostructure with 16 Li atoms.

| Method | $\mu_{Li}$, eV/at. | $E_i$, eV/at. | $e^-$ from Li |
|---|---|---|---|
| DFT-D2[38] | -2.02 | -0.47 | 0.84 |
| DFT-D3[39] | -2.00 | -0.16 | 0.84 |
| DFT-D3-BJ[40] | -2.07 | -0.18 | 0.83 |
| DFT-TS[42] | -4.14 | 1.01 | 0.83 |
| DFT-TS/HI[51] | -4.02 | 1.91 | 0.84 |
| DFT-dDsC[43] | -1.97 | -0.08 | 0.84 |
| optB86b-vdW[47] | -1.54 | -0.17 | 0.84 |
| optB88-vdW[47] | -1.51 | -0.21 | 0.84 |
| optPBE-vdW[47] | -1.49 | -0.12 | 0.84 |
| rev-vdW-DF2[52] | -1.60 | -0.19 | 0.84 |
| SCAN-rVV10[48] | -2.28 | -0.27 | 0.85 |
| vdW-DF2[53] | -1.41 | -0.32 | 0.83 |
| vdW-DF[45] | -1.48 | 0.12 | 0.84 |

Having tested the vdW methods in the context of intercalation simulations, we first studied what positions of AMs are energetically more favorable and assessed the energetics of AM atoms between $Gr/MoS_2$ sheets in the single-layer configuration. It was previously shown[27] that in bilayer graphene with different stacking (AA-stacking and AB-stacking) the formation of a single layer system with a geometry close to the $C_6LiC_6$ configuration with Li atoms being on top of the hexagons is possible. Here we found that Li atoms take positions on top of the Mo atoms, in agreement with the results of a previous study.[18]

To find out the relationship between the energetics and concentration of AM atoms, and determine the most energetically favorable concentrations of Li, Na, K atoms in the $Gr/MoS_2$ heterostructure, we calculated the total energy of the system with an increasing number $n$ of AM atoms and computed $E_i$ and $E_r$ as functions of AM atom concentration $x = n_{AM}/n_{Mo}$, where $n_{Mo}$ is the total number number of Mo atoms in the supercell ($n_{Mo} = 16$ in our calculations). Fig. 2 shows the changes in $E_i$ and $E_r$ with increasing $x$. We would like to

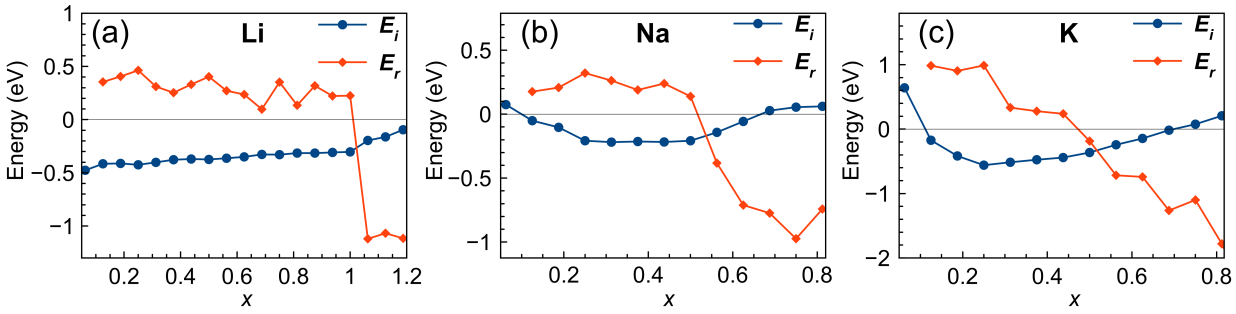


Figure 2: Intercalation energy $E_i$ and reaction energy $E_r$ as functions of AM atom concentration $x = n_{AM}/N_{Mo}$ for Li (a), Na (b), and K (c) atoms intercalated as a single layer into a Gr/H-$MoS_2$ bilayer heterostructure.

reiterate here that positive values of $E_i$ indicate that intercalation is energetically unfavorable (although still possible if a voltage is applied to the system), and negative values of $E_r$ indicate that segregation of the intercalated atoms into areas with different concentrations should be expected. In the case of Li, the maximum possible concentration of AM atoms in Gr/$MoS_2$ heterostructure is $x = 1.00$ (16 Li atoms per 16 Mo atoms), as $E_r < 0$ for higher concentrations, although $E_i$ remains negative even at the highest concentration studied, Fig. 2(a). This result is in a good agreement with the previously reported data.[18] The Gr/$MoS_2$ heterostructure can accommodate twice the number of Li atoms as compared to bi-layer graphene.[54] As discussed previously,[54] the presence of the graphene layer makes the intercalated system more stable and allows cycling of Li without formation of lithium sulfide.

In the case of Na, the maximum possible concentration of AM atoms in Gr/$MoS_2$ heterostructure is $x = 0.56$, Fig. 2(b), the maximum possible concentration of K is $x = 0.5$, Fig. 2(c). This can be associated with larger atomic radii of Na and K as compared to Li. We investigated the intercalation of Na and K in the Gr/$MoS_2$ heterostructure with $x$ up to unity, but we found that for concentrations above $x \sim 0.81$ Na and K atoms form two-layer structures instead of the single-layer one, and therefore the results for $x > 0.81$ are not included in the plots.

As shown in previous theoretical[55–57] and experimental[4,58,59] studies, an increase in Li concentration in pure $MoS_2$ causes a transition from the trigonal H phase to an octahedral

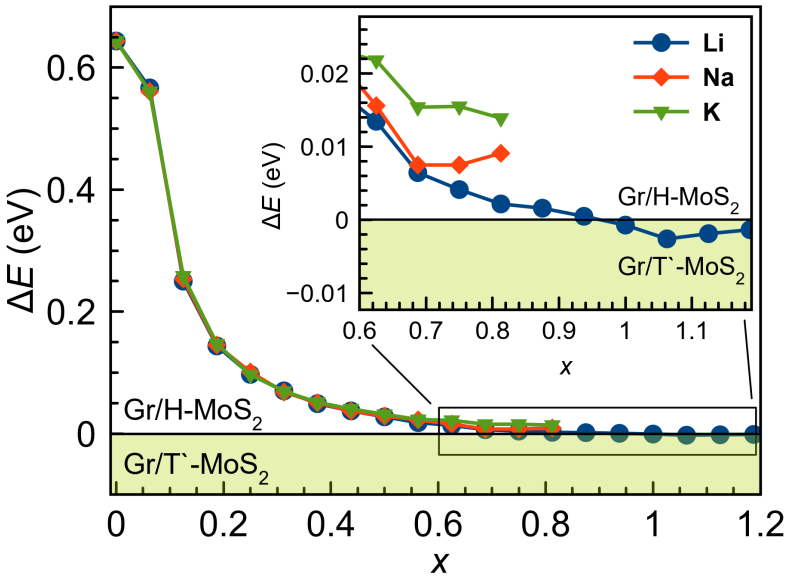


Figure 3: Difference in the total energy of Gr/H-$MoS_2$ and Gr/T′-$MoS_2$ heterostructures with intercalated AM atoms as a function of AM concentration.

$T$-phase and then to a distorted $T'$-phase. The transition from the $H$ phase to the distorted T′ phases is associated with a substantial energy barrier which is considerably reduced by increasing the concentration of Li atoms. It is important to note that H-$MoS_2$ layer is a semiconductor, whereas T′-$MoS_2$ is a metallic system. To understand what would happen in the Gr/$MoS_2$ heterostructure, we studied the influence of AM concentration on the energetics of the H and T′ phases in the Gr/$MoS_2$ structure. To do so, we also considered intercalated AMs in Gr/T′-$MoS_2$ and calculated the energy difference $\Delta E$ between the Gr/H-$MoS_2$ and Gr/T′-$MoS_2$ heterostructures for each concentration of AMs. Fig. 3 shows the dependence of $\Delta E$ on the concentration of Li, Na, and K atoms in the Gr/$MoS_2$ heterostructure with the $MoS_2$ sheet being in the H or T′ phase. As evident from the figure, in case of Li at concentration $x \sim 1$, the T′-phase becomes more energetically favorable than the H-phase. Upon Na and K intercalation, the H phase always remains preferable.

This phase transition from the H to the T′ phase is associated with charge transfer from Li atoms to the $MoS_2$ layer. It was theoretically demonstrated[56] that in the free-standing $MoS_2$ monolayer the phase transition occurs at Li concentration of about $x = 0.4$ (note that

as adsorption of Li atoms on both sides of the $MoS_2$ layer was considered in that paper, which increased the number of possible adsorption sites by a factor of two, the concentration defined in our work should be divided by two for a comparison with the results presented in Ref.[56]) and each Li atom donates approximately 0.8 electrons to the $MoS_2$ monolayer. Thus 0.32e per Mo atom should be sufficient for the transformation. In our simulations only one side of $MoS_2$ is in contact with Li, and the charge which is donated by Li atoms is shared between the graphene and $MoS_2$ layers. We found that Li atoms intercalated between graphene and $MoS_2$ layer donate approximately 0.8 electrons, Fig. 4(a,b), $0.5e$ of which is accumulated on $MoS_2$ and $0.3e$ on graphene, in agreement with the previous studies.[17,18] The transition from the H to the T′ phase was found to occur at $x \sim 0.94$, which gives about 0.46e per Mo atom, a value close but slightly higher than what was reported for $MoS_2$ monolayer.

Using the Bader method, we extended the charge transfer analysis to K and Na. Figs. 4(c,d) show the dependence of the charge transfer from the AM atoms to graphene and $MoS_2$ on AM atom concentration. In the case of Na, at a concentration ranging from 0.25 to 0.45 we observed the maximum number of electrons donated by Na (0.82e) which matches the minimum of intercalation energy for this concentration, Fig. 2(b). Similar to Na, in the case of K the maximum number of electrons which leave K atoms (0.85e, at $x = 0.25$) also matches the minimum of $E_i$, Fig. 2(c). In all systems (except for the case with one AM atom in the Gr/H-$MoS_2$ heterostructure) more electrons are accumulated in the $MoS_2$.

To get a better understanding of the spatial redistribution of charge upon intercalation, we calculated the electron density difference $\Delta\rho$ (the density of the combined system minus the sum of the densities of the isolated heterostructure and single layer AM atoms with the same atom positions as in the combined system) for single layers of AM atoms with different concentrations averaged in the planes parallel to the Gr/$MoS_2$ sheets as a function of the $z$-coordinate. The averaging was done by integrating the electron density within the plane parallel to the Gr/$MoS_2$ sheets. The results for Na are presented in Fig. 5. for different

concentrations corresponding to the number of AM atoms in the supercell ranging from 1 to 13. Areas below zero correspond to the depletion of electron density, above zero stand for density build-up. It is evident that the transferred charge is spatially localized mostly next to the S-layer of $MoS_2$ facing the AM atoms. According to these calculations, the charge accumulation, which can be associated with chemical bonding between Na atoms and $MoS_2$, is always larger than with graphene except for the case of one AM atom between Gr/H-$MoS_2$. We received qualitatively similar results for other AM we considered (see SI).

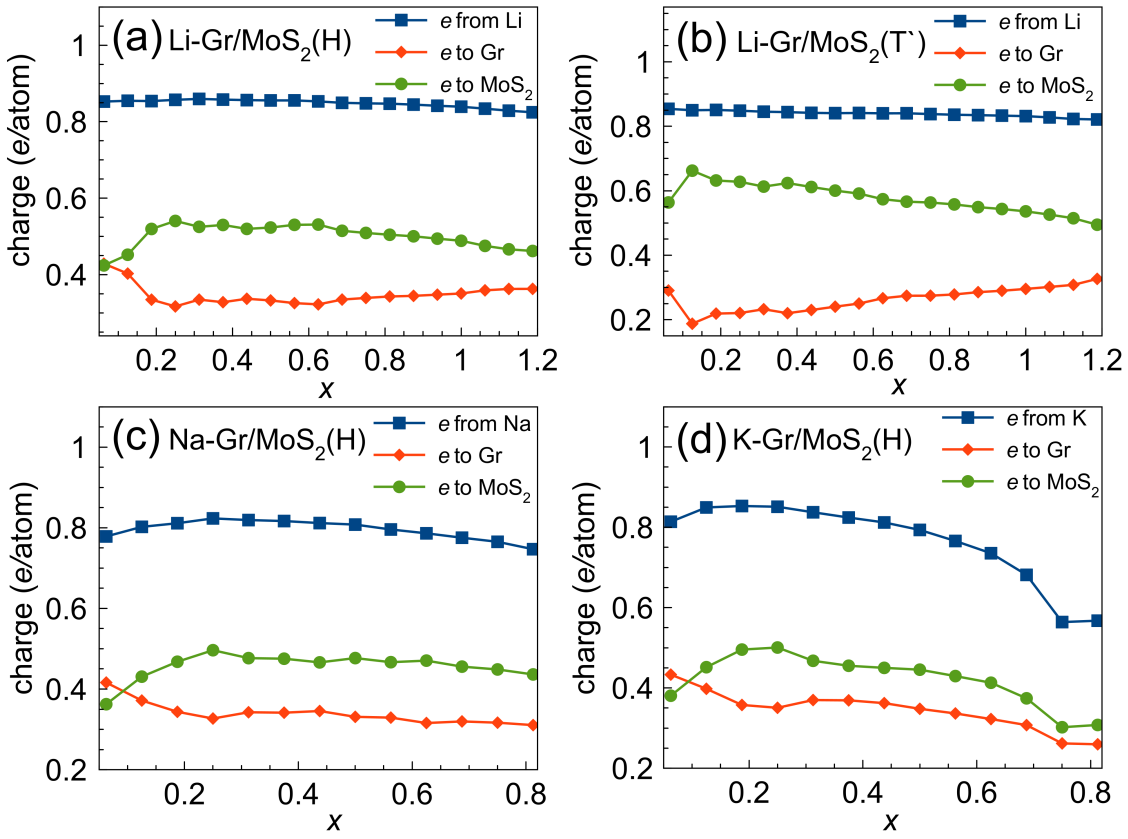


Figure 4: Charge transfer between the intercalated AM atoms and the host structure as a function of the concentration of AM atoms calculated using the Bader method for Li (a, b), Na (c), and K (d) for the Gr/H-$MoS_2$ and Gr/T′-$MoS_2$ heterostructures.

Since previous experimental[27] and theoretical [28] data indicated that formation of multilayers of AM atoms in bilayers of graphene and $MoS_2$ is possible, we also studied AM multi-layers in the Gr/H-$MoS_2$ heterostructure. To determine the most energetically favor-

able configurations of AM multilayers, we considered different initial structures of the AM atoms. Initial atom positions were cut from the bulk fcc, hcp, bcc metals along the low-energy directions (e.g. [111] for the fcc structures) and placed between the graphene and $MoS_2$ layers. The orientation of the metal crystal lattice with regard to graphene/$MoS_2$ and the sizes of the supercells were chosen to minimize the strain in the system. The strain normally did not exceed 1%. We calculated the intercalation energy and charge transfer for two, three and four layers of Li,Na, K in Gr/H-$MoS_2$ and Gr/T′-$MoS_2$ heterostructures. The intercalation energy as a function of AM atom concentration for single- and multi-layer structures is shown in Fig. 6(a-c). In the case of Li, the intercalation energy is negative, which means that these structures can be formed. For Na, it is interesting that the intercalation energy for bcc and hcp multi-layers is negative and is roughly the same as for one layer of Na with a concentration of atoms above 0.6. These results indicate that the formation of Na multilayers in the Gr/$MoS_2$ is possible for high concentration of Na atoms. The same results were obtained for K, but for different structures - bcc and fcc.

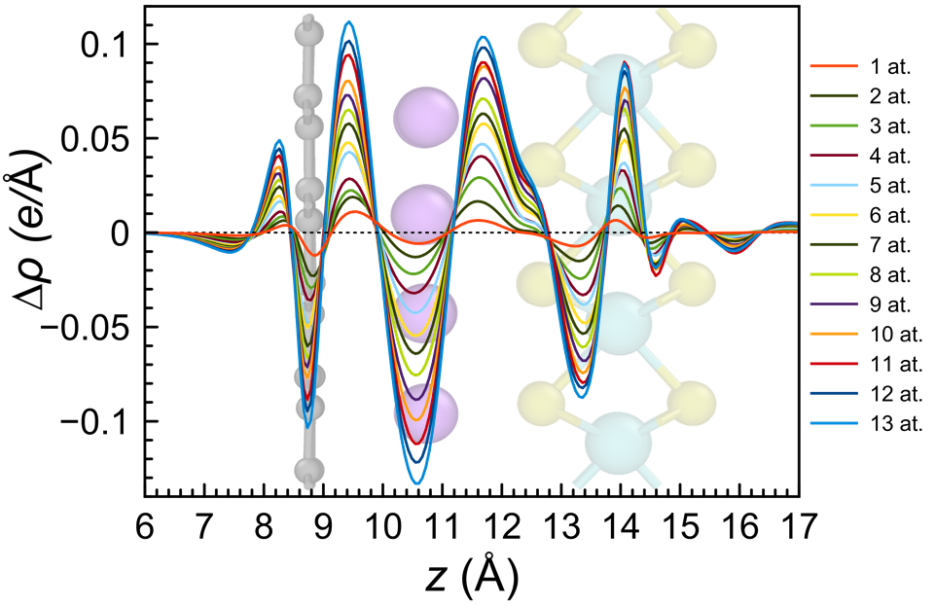


Figure 5: Electron density difference $\Delta\rho$ for a single layer of Na atoms with different concentrations (number of atoms) averaged in the planes parallel to the Gr/$MoS_2$ sheets as a function of the z-coordinate (perpendicular to the planes). The positions of the atoms are schematically shown.

As we showed previously for the intercalation of Li, see Figs. 3 and 4(a), the T′ phase becomes energetically favorable in $MoS_2$ at about 0.5 electrons per $MoS_2$ cell, so that it can also exist in multi-layer structures. As seen from Fig. 6(d), only in the case of Li, the multilayers (in bcc and hcp case) donate the needed number of electrons to $MoS_2$. We compared the intercalation energy of all structures of Li multilayers between Gr/H-$Mos_2$ and Gr/T′-$MoS_2$ and observed that in the case of bcc and fcc configurations the T′- phase is more energetically favorable. These results show that if multi-layer Li structures are formed, the phase transition from H to T′ in $MoS_2$ layer should indeed take place. Multilayers of Na and K do not donate enough electrons for the transition, Fig. 6(e,f), in agreement with our calculations of the total energies of the systems, which indicate that the H phase has lower energy.

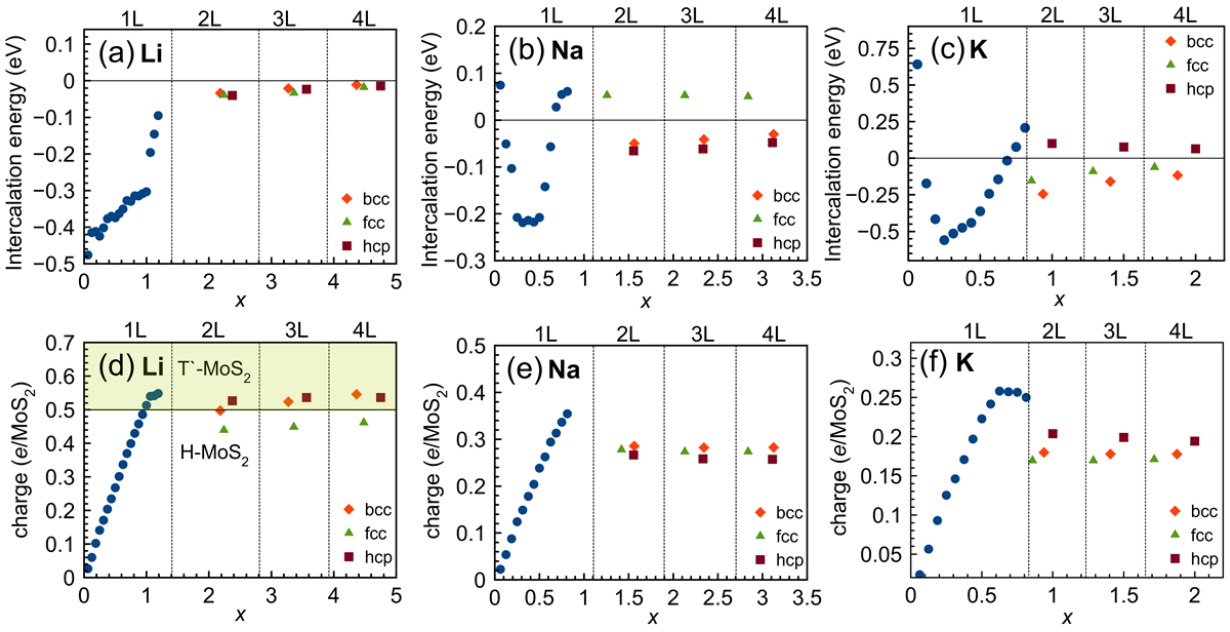


Figure 6: Intercalation energy as a function of the concentration of Li (a), Na (b) and K (c) atoms in single (1L), double (2L), and multi-layer (3L and 4L) configurations in the Gr/H-$MoS_2$ heterostructure. (d-f) - Corresponding charge transferred to $MoS_2$ sheet in the heterostructure.

# Conclusions

To sum up, using DFT calculations, we systematically studied the intercalation of Li, Na, K atoms into a graphene/$MoS_2$ heterostructure. We considered not only single-, but also multi-layer configurations of AM atoms, which have not been investigated before. We assessed the intercalation energetics for various concentrations of AM atoms, calculated charge transfer from AM atoms to the host system, and showed that although intercalation of AMs as single layer is overall energetically preferable, multi-layer configurations can exist at high concentrations of AM atoms. We further demonstrated that the transition of the $MoS_2$ layer from the $H$ to $T'$ phase is possible upon Li intercalation, but not for Na or K.

The simulations performed in this work were motivated by recent technical advances based on a peripheral galvanic cell geometry and Hall voltammetry that allow the study of intercalant motion, diffusion and ordering without the complications brought by the solid electrolyte interface in standard conventional battery cells.[27,60] The simulations offer important guidance as to which intercalants and heterointerfaces may be beneficial for further experimental explorations that aim at identifying systems with excellent mixed conductor properties as required for efficient anodes. Structural phase transformations may hamper reversibility and the awareness of their existence or absence is therefore valuable in the selection of promising intercalant/heterointerface combinations.

Overall, we expect that our results should help one to better understand the behavior of heterostructures assembled from 2D materials upon AM atom intercalation. We also envisage that our findings may stimulate further experimental effort focused on the tailoring of the electronic properties of such heterostructures. Moreover, the results of our simulations should be beneficial for increasing the capacity of anode materials in AM ion batteries.

# Associated Content

The Supporting Information is available free of charge at https://pubs.acs.org/doi/10.1021/XXXXXX.

The Supporting Information reports the parameters of the supercells used and the results of additional calculations are also presented.

## Acknowledgement

We thank Dr. M. Ghorbani-Asl for fruitful discussions. AVK acknowledges the German Research Foundation (DFG) for the support through Project KR 4866/6-1 and the collaborative research center "Chemistry of Synthetic 2D Materials" SFB-1415-417590517. JHS acknowledges financial support from the EU graphene flagship core 3 program. IVC thanks the German Academic Exchange Service (DAAD) program "Mikhail Lomonosov" for support. The authors thank the HZDR Computing Center, HLRS, Stuttgart, Germany, and TU Dresden Cluster "Taurus" for generous grants of CPU time.

## References

(1) Xu, J.; Dou, Y.; Wei, Z.; Ma, J.; Deng, Y.; Li, Y.; Liu, H.; Dou, S. Recent Progress in Graphite Intercalation Compounds for Rechargeable Metal (Li, Na, K, Al)-Ion Batteries. *Advanced Science* **2017**, *4*, 1700146.

(2) Ji, K.; Han, J.; Hirata, A.; Fujita, T.; Shen, Y.; Ning, S.; Liu, P.; Kashani, H.; Tian, Y.; Ito, Y. et al. Lithium intercalation into bilayer graphene. *Nature Communications* **2019**, *10*, 275.

(3) Sonia, F. J.; Jangid, M. K.; Ananthoju, B.; Aslam, M.; Johari, P.; Mukhopadhyay, A. Understanding the Li-storage in few layers graphene with respect to bulk graphite: experimental, analytical and computational study. *Journal of Materials Chemistry A* **2017**, *5*, 8662–8679.

(4) Bediako, D. K.; Rezaee, M.; Yoo, H.; Larson, D. T.; Zhao, S.; Taniguchi, T.; Watan-

abe, K.; Brower-Thomas, T. L.; Kaxiras, E.; Kim, P. Heterointerface effects in the electrointercalation of van der Waals heterostructures. *Nature* **2018**, *558*, 425–429.

(5) Ichinokura, S.; Sugawara, K.; Takayama, A.; Takahashi, T.; Hasegawa, S. Superconducting calcium-intercalated bilayer graphene. *Acs Nano* **2016**, *10*, 2761–2765.

(6) Durajski, A. P.; Skoczylas, K. M.; Szcześniak, R. Superconductivity in bilayer graphene intercalated with alkali and alkaline earth metals. *Physical Chemistry Chemical Physics* **2019**, *21*, 5925–5931.

(7) Liu, C.; Bai, Y.; Zhao, Y.; Yao, H.; Pang, H. MoS2/graphene composites: Fabrication and electrochemical energy storage. *Energy Storage Materials* **2020**, *33*, 470–502.

(8) Shiva, K.; Ramakrishna Matte, H. S.; Rajendra, H. B.; Bhattacharyya, A. J.; Rao, C. N. Employing synergistic interactions between few-layer WS2 and reduced graphene oxide to improve lithium storage, cyclability and rate capability of Li-ion batteries. *Nano Energy* **2013**, *2*, 787–793.

(9) Thanh, T. D.; Chuong, N. D.; Van Hien, H.; Kshetri, T.; Kim, N. H.; Lee, J. H. Recent advances in two-dimensional transition metal dichalcogenides-graphene heterostructured materials for electrochemical applications. *Progress in Materials Science* **2018**, *96*, 51–85.

(10) Huang, Z.; Han, X.; Cui, X.; He, C.; Zhang, J.; Wang, X.; Lin, Z.; Yang, Y. Vertically aligned VS 2 on graphene as a 3D heteroarchitectured anode material with capacitance-dominated lithium storage. *Journal of Materials Chemistry A* **2020**, *8*, 5882–5889.

(11) Chang, K.; Chen, W. In situ synthesis of MoS2/graphene nanosheet composites with extraordinarily high electrochemical performance for lithium ion batteries. *Chemical Communications* **2011**, *47*, 4252–4254.

(12) Chang, K.; Chen, W. L-cysteine-assisted synthesis of layered MoS2/graphene composites with excellent electrochemical performances for lithium ion batteries. *ACS Nano* **2011**, *5*, 4720–4728.

(13) Chang, K.; Chen, W.; Ma, L.; Li, H.; Li, H.; Huang, F.; Xu, Z.; Zhang, Q.; Lee, J.-Y. Graphene-like MoS 2/amorphous carbon composites with high capacity and excellent stability as anode materials for lithium ion batteries. *Journal of Materials Chemistry* **2011**, *21*, 6251–6257.

(14) Pushparaj, R. I.; Cakir, D.; Zhang, X.; Xu, S.; Mann, M.; Hou, X. Coal-Derived Graphene/MoS2 Heterostructure Electrodes for Li-Ion Batteries: Experiment and Simulation Study. *ACS Applied Materials & Interfaces* **2021**, *13*, 59950–59961.

(15) Miwa, R. H.; Scopel, W. L. Lithium incorporation at the MoS2/graphene interface: an ab initio investigation. *Journal of Physics: Condensed Matter* **2013**, *25*, 445301.

(16) Ahmed, T.; Modine, N.; Zhu, J.-X. Bonding between graphene and MoS2 monolayers without and with Li intercalation. *Applied Physics Letters* **2015**, *107*, 043903.

(17) Shao, X.; Wang, K.; Pang, R.; Shi, X. Lithium intercalation in graphene/MoS2 composites: first-principles insights. *The Journal of Physical Chemistry C* **2015**, *119*, 25860–25867.

(18) Larson, D. T.; Fampiou, I.; Kim, G.; Kaxiras, E. Lithium intercalation in graphene–MoS2 heterostructures. *The Journal of Physical Chemistry C* **2018**, *122*, 24535–24541.

(19) Sun, D.; Ye, D.; Liu, P.; Tang, Y.; Guo, J.; Wang, L.; Wang, H. MoS2/Graphene nanosheets from commercial bulky MoS2 and graphite as anode materials for high rate sodium-Ion batteries. *Advanced Energy Materials* **2018**, *8*, 1702383.

(20) Li, G.; Luo, D.; Wang, X.; Seo, M. H.; Hemmati, S.; Yu, A.; Chen, Z. Enhanced

Reversible Sodium-Ion Intercalation by Synergistic Coupling of Few-Layered MoS2 and S-Doped Graphene. *Advanced Functional Materials* **2017**, *27*, 1702562.

(21) David, L.; Bhandavat, R.; Singh, G. MoS2/graphene composite paper for sodium-ion battery electrodes. *ACS nano* **2014**, *8*, 1759–1770.

(22) Xie, X.; Ao, Z.; Su, D.; Zhang, J.; Wang, G. MoS2/graphene composite anodes with enhanced performance for sodium-ion batteries: the role of the two-dimensional heterointerface. *Advanced Functional Materials* **2015**, *25*, 1393–1403.

(23) Massaro, A.; Pecoraro, A.; Muñoz-García, A. B.; Pavone, M. First-Principles Study of Na Intercalation and Diffusion Mechanisms at 2D MoS2/Graphene Interfaces. *The Journal of Physical Chemistry C* **2021**, *125*, 2276–2286.

(24) Wang, B.; Peng, Y.; Yuan, F.; Liu, Q.; Sun, L.; Zhang, P.; Wang, Q.; Li, Z.; Wu, Y. A. A comprehensive review of carbons anode for potassium-ion battery: Fast kinetic, structure stability and electrochemical. *Journal of Power Sources* **2021**, *484*, 229244.

(25) Zhang, J.; Lai, L.; Wang, H.; Chen, M.; Shen, Z. X. Energy storage mechanisms of anode materials for potassium ion batteries. *Materials Today Energy* **2021**, 100747.

(26) Zhang, P.; Yang, Y.; Duan, X.; Zhao, S.; Lu, C.; Shen, Y.; Shao, G.; Wang, S. Mechanistic investigations of N-doped graphene/2H(1T)-MoS2 for Li/K-ions batteries. *Nano Energy* **2020**, *78*, 105352.

(27) Kühne, M.; Börrnert, F.; Fecher, S.; Ghorbani-Asl, M.; Biskupek, J.; Samuelis, D.; Krasheninnikov, A. V.; Kaiser, U.; Smet, J. H. Reversible superdense ordering of lithium between two graphene sheets. *Nature* **2018**, *564*, 234—239.

(28) Chepkasov, I. V.; Ghorbani-Asl, M.; Popov, Z. I.; Smet, J. H.; Krasheninnikov, A. V. Alkali metals inside bi-layer graphene and MoS2: Insights from first-principles calculations. *Nano Energy* **2020**, *75*, 104927.

(29) Kresse, G.; Furthmüller, J. Efficient iterative schemes for ab initio total-energy calculations using a plane-wave basis set. *Physical Review B* **1996**, *54*, 11169.

(30) Kresse, G.; Joubert, D. From ultrasoft pseudopotentials to the projector augmented-wave method. *Physical Review B* **1999**, *59*, 1758.

(31) Monkhorst, H. J.; Pack, J. D. Special points for Brillouin-zone integrations. *Physical Review B* **1976**, *13*, 5188.

(32) Momma, K.; Izumi, F. VESTA: a three-dimensional visualization system for electronic and structural analysis. *Journal of Applied Crystallography* **2008**, *41*, 653–658.

(33) Smidstrup, S.; Markussen, T.; Vancraeyveld, P.; Wellendorff, J.; Schneider, J.; Gunst, T.; Verstichel, B.; Stradi, D.; Khomyakov, P. A.; Vej-Hansen, U. G. et al. QuantumATK: An integrated platform of electronic and atomic-scale modelling tools. *Journal of Physics: Condensed Matter* **2019**, *32*, 015901.

(34) Björkman, T.; Gulans, A.; Krasheninnikov, A. V.; Nieminen, R. M. van der Waals bonding in layered compounds from advanced density-functional first-principles calculations. *Physical Review Letters* **2012**, *108*, 235502.

(35) Björkman, T.; Gulans, A.; Krasheninnikov, A.; Nieminen, R. Are we van der Waals ready? *Journal of Physics: Condensed Matter* **2012**, *24*, 424218.

(36) Tawfik, S. A.; Gould, T.; Stampfl, C.; Ford, M. J. Evaluation of van der Waals density functionals for layered materials. *Physical Review Materials* **2018**, *2*, 034005.

(37) Li, J.; Kolekar, S.; Ghorbani-Asl, M.; Lehnert, T.; Biskupek, J.; Kaiser, U.; Krasheninnikov, A. V.; Batzill, M. Layer-Dependent Band Gaps of Platinum Dichalcogenides. *ACS Nano* **2021**, *15*, 13249–13259.

(38) Grimme, S. Semiempirical GGA-type density functional constructed with a long-range dispersion correction. *Journal of Computational Chemistry* **2006**, *27*, 1787–1799.

(39) Grimme, S.; Antony, J.; Ehrlich, S.; Krieg, H. A consistent and accurate ab initio parametrization of density functional dispersion correction (DFT-D) for the 94 elements H-Pu. *The Journal of Chemical Physics* **2010**, *132*, 154104.

(40) Grimme, S.; Ehrlich, S.; Goerigk, L. Effect of the damping function in dispersion corrected density functional theory. *Journal of computational chemistry* **2011**, *32*, 1456–1465.

(41) Tkatchenko, A.; DiStasio Jr, R. A.; Car, R.; Scheffler, M. Accurate and efficient method for many-body van der Waals interactions. *Physical Review Letters* **2012**, *108*, 236402.

(42) Tkatchenko, A.; Scheffler, M. Accurate molecular van der Waals interactions from ground-state electron density and free-atom reference data. *Physical Review Letters* **2009**, *102*, 073005.

(43) Steinmann, S. N.; Corminboeuf, C. A generalized-gradient approximation exchange hole model for dispersion coefficients. *The Journal of Chemical Physics* **2011**, *134*, 044117.

(44) Gould, T.; Lebegue, S.; Ángyán, J. G.; Bucko, T. A fractionally ionic approach to polarizability and van der Waals many-body dispersion calculations. *Journal of Chemical Theory and Computation* **2016**, *12*, 5920–5930.

(45) Dion, M.; Rydberg, H.; Schröder, E.; Langreth, D. C.; Lundqvist, B. I. Van der Waals density functional for general geometries. *Physical Review Letters* **2004**, *92*, 246401.

(46) Klimeš, J.; Bowler, D. R.; Michaelides, A. Van der Waals density functionals applied to solids. *Physical Review B* **2011**, *83*, 195131.

(47) Klimeš, J.; Bowler, D. R.; Michaelides, A. Chemical accuracy for the van der Waals density functional. *Journal of Physics: Condensed Matter* **2009**, *22*, 022201.

(48) Peng, H.; Yang, Z.-H.; Perdew, J. P.; Sun, J. Versatile van der Waals density functional based on a meta-generalized gradient approximation. *Physical Review X* **2016**, *6*, 041005.

(49) Park, J.; Yu, B. D.; Hong, S. Van der Waals density functional theory study for bulk solids with BCC, FCC, and diamond structures. *Current Applied Physics* **2015**, *15*, 885–891.

(50) Tang, W.; Sanville, E.; Henkelman, G. A grid-based Bader analysis algorithm without lattice bias. *Journal of Physics: Condensed Matter* **2009**, *21*, 084204.

(51) Bucko, T.; Lebegue, S.; Hafner, J.; Angyan, J. G. Improved density dependent correction for the description of London dispersion forces. *Journal of Chemical Theory and Computation* **2013**, *9*, 4293–4299.

(52) Hamada, I. van der Waals density functional made accurate. *Physical Review B* **2014**, *89*, 121103.

(53) Lee, K.; Murray, É. D.; Kong, L.; Lundqvist, B. I.; Langreth, D. C. Higher-accuracy van der Waals density functional. *Physical Review B* **2010**, *82*, 081101.

(54) Shirodkar, S. N.; Kaxiras, E. Li intercalation at graphene/hexagonal boron nitride interfaces. *Physical Review B* **2016**, *93*, 245438.

(55) Nasr Esfahani, D.; Leenaerts, O.; Sahin, H.; Partoens, B.; Peeters, F. Structural transitions in monolayer MoS2 by lithium adsorption. *Journal of Physical Chemistry C* **2015**, *119*, 10602–10609.

(56) Kan, M.; Wang, J.; Li, X.; Zhang, S.; Li, Y.; Kawazoe, Y.; Sun, Q.; Jena, P. Structures and phase transition of a MoS2 monolayer. *The Journal of Physical Chemistry C* **2014**, *118*, 1515–1522.

(57) Kretschmer, S.; Komsa, H.-P.; Bøggild, P.; Krasheninnikov, A. V. Structural Transformations in Two-Dimensional Transition-Metal Dichalcogenide MoS2 under an Electron Beam: Insights from First-Principles Calculations. *The Journal of Physical Chemistry Letters* **2017**, *8*, 3061–3067.

(58) Kim, J. S.; Kim, J.; Zhao, J.; Kim, S.; Lee, J. H.; Jin, Y.; Choi, H.; Moon, B. H.; Bae, J. J.; Lee, Y. H. et al. Electrical Transport Properties of Polymorphic MoS2. *ACS Nano* **2016**, *10*, 7500–7506.

(59) Kappera, R.; Voiry, D.; Yalcin, S. E.; Branch, B.; Gupta, G.; Mohite, A. D.; Chhowalla, M. Phase-engineered low-resistance contacts for ultrathin MoS2 transistors. *Nature Materials* **2014**, *13*, 1128–1134.

(60) Kühne, M.; Paolucci, F.; Popovic, J.; Ostrovsky, P. M.; Maier, J.; Smet, J. H. Ultrafast lithium diffusion in bilayer graphene. *Nature Nanotechnology* **2017**, *12*, 895–900.

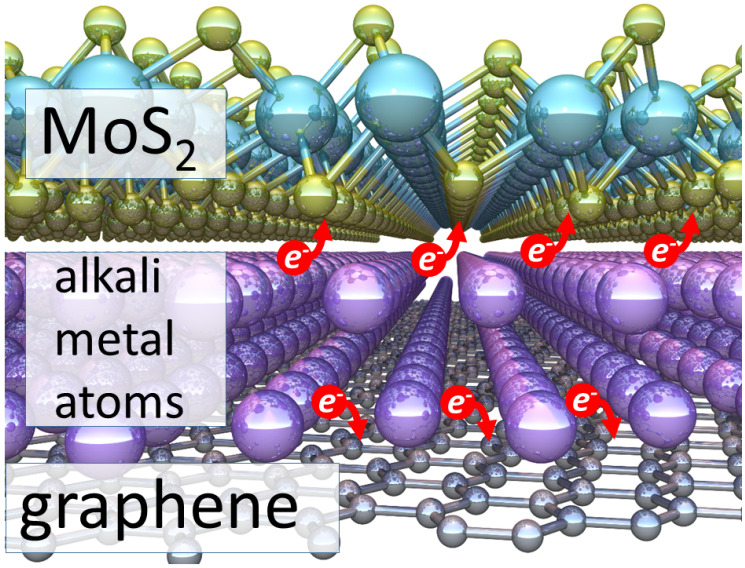


TOC figure